Support Tucker Machines Based Bubble Defect Detection of Lithium-ion Polymer Cell Sheets

Liyong Ma, *Member, IAENG,* Yuehong Hu, and Yong Zhang

***Abstract*—Recently Lithium-ion polymer (LiPo) battery attracts more interests in both technology and application for its high energy density and easy to be manufactured in different shapes. The LiPo battery quality is essential for all the applications, and the defect detection of LiPo cell sheets in the automatic production line is critical to battery quality control. After capturing the images of two sides of LiPo cell sheets with controlled manipulators in the automatic line, support Tucker machines (STM) method based on the tensor is applied to detect bubble defects in Lithium-ion polymer cell sheets. The preprocessing of the cell sheet images and the proposed STM based method are detailed. The experimental results demonstrate that the proposed STM based bubble defect detection method is more efficient than other common learning based methods, and the proposed STM based method is potential for classification in image applications.**

***Index Terms*—Support Tucker machines, defect detection, machine vision, Lithium-ion polymer battery**

I. Introduction

BATTERIES have been widely used in our everyday life, for example, from the mobile phone to the vehicles, even the submarine. After the development in the past 20 years, rechargeable battery has made considerable progress in providing increasingly greater density and energy per volume, longer cycle life and higher reliability [1]. As a kind of lithium-ion based rechargeable battery, lithium-ion polymer (LiPo) battery with a lot of advantages attracts more interests in both technology and application. At first, LiPo battery has the same advantages with the lithium-ion battery. These advantages include higher energy density, no memory effect, and slow charge loss during free time. Meanwhile, LiPo battery is produced with a soft package or pouch, which makes the battery lighter than common lithium-ion battery. LiPo battery can also be thin, flexible, and manufactured in different shapes, without risk of electrolyte leakage. Another compelling advantage of LiPo battery is that it can be shaped to different shapes. This is important to applications requiring a small footprint for the energy storage system. And it makes LiPo battery more suitable for thinner and lighter portable applications than other batteries. Apart from the consumer electrical and electronic devices including mobile phones, digital cameras and laptops, a diversity of electronic and electrical devices are powered by LiPo batteries now. For example, these devices include patient monitor, portable diagnosis equipment, automotive, and industrial equipment, et al.

The LiPo battery quality is essential for all the applications. To improve the quality of the LiPo batteries, automatic line has been adopted in many factories. Recently an automatic LiPo battery line is developed to employ some novel manufacture techniques for TSE Technology Corporation in Weihai, China. This production process of the LiPo batteries includes several stages. Firstly, the battery pole pieces and separators are produced. Subsequently several pole pieces and separators are employed to produce cell sheets with heat sealing technique. Lastly, these cell sheets are stacked together to form galvanic piles and provide various battery capacities. The quality evaluation of cell sheets in the automatic line is critical to battery quality control during the production period. Some quality tests of the cell sheets are used, for example, short circuit test and breakdown test. The surface defect detection has to be employed to avoid the damaging or out-of-flatness of the cell sheet net. This work is inefficient and hard labor when it is performed manually. In this paper, after collecting the images of the cell sheets by machine vision technique, an automatic image processing technique is proposed to defect detection of the cell sheets.

Machine vision has been widely used in a variety of applications. Bu et al reported the defect detection of the fabric using support vector data description [2]. In food field, biscuits crack inspection is performed with machine vision [3]. In IC industry, machine vision is employed for defect detection [4]. In solar industry, mirco-crack inspections of the solar wafers and the solar cells are reported [5].

Some common learning based algorithms have been reported on these defect detection applications. Neural network based methods had been used in texture surface classification [6]. The Support Vector Machines (SVM) was proposed to solve the two-class problem [7]. With the performance prior to neural network and other methods, SVM has the potential to solve the classification problems of small samples, nonlinearity and the curse of dimension [8]-[11]. Therefore it has been widely used for pattern classification and regression problem [7]-[11]. However, we often use vectors to describe every image in the image classification applications using SVM, which leads to a large vector space problem produced by the training data. It

Manuscript received June 11, 2016; revised January 13, 2017. This work was supported in part by National Natural Science Foundation of China (61371045), Science and Technology Development Plan Project of Shandong Province, China (2015GGX103016).

Liyong Ma is with School of Information & Electrical Enginneing, Harbin Institute of Technology, Weihai, 264209, China (phone: +86-631-2679199; e-mail: maliyong@hit.edu.cn).

Yuehong Hu and Yong Zhang are with Harbin Institute of Technology, Weihai, 264209, China (e-mail: huyuehong@ghtt.net, zy7954@yeah.net).

consumes long time for computing and may damage the two-dimensional structure of the image matrix. In order to avoid the data destruction by converting tensors into vectors, the supervised tensor learning method is proposed [12]-[13]. In this method, the Tucker tensor decomposition is employed to decompose a tensor into a core tensor multiplied by a matrix along each mode. The advantage of this method is that the parameters of weights can form a tensor. While we use the images as a tensor form directly, the structure of the image is effectively retained. Thus it will make image processing more intuitively and correctly. This method has been employed in marine oil spill detection with SAR images as reported in [14].

In this letter, we detect bubble defects in LiPo cell sheets employing support Tucker machines (STM) method based on the tensor. The details of obtaining a tensor formed by the weights parameters through the Tucker tensor decomposition are discussed. This letter is organized as follows. After the background introduction, machine vision based image capture method of LiPo cell sheets is described in Section II. Support Tucker machines are discussed in Section III, and our proposed STM based bubble defect detection algorithm for LiPo cell sheets is detailed in Section IV. The experimental results are discussed in Section V and the conclusion is given in the last.

II. Image Capture of LIPO Celle Sheets

The images of the LiPo cell sheets are captured from the automatic line which has been developed in TSE Technology Corporation. Special LiPo battery product technique has been developed in this automatic line. In this technique, the LiPo battery pole pieces and the LiPo battery separators are sealed together with heat sealing method to form cell sheets. With these new techniques, the LiPo battery products have quite a few advantages. Galvanic pile is formed through overlapping of monolithic cell sheets, which brings the large room for capacity design. Meanwhile, the product is fairly safer than other similar products while using phase separation to make non free-state electrolyte to exist in the space. Specially designed negative materials and formula of metallic grid electrode adhesive have some advantages, for example easy to mix electrode materials, reduce internal resistance and increase the adhesive strength of basic materials. It can adapt to the working environment during charging or discharging under high current, which can greatly increase battery's circle life. The special technology of separator can improve the safety and function of LiPo battery and the compatibility of the electrolyte. And it makes battery magnification rise of 10%-20%, and provides good performance in the environment of either high temperature or low temperature. On the other hand the detection of the quality of product and material is critical during the manufacture to ensure the product can provide improved performance and enhanced safety. Therefore the defect detection is essential in the automatic production line. Traditional detection cannot meet the requirement of these advanced techniques for cell production. A novel inspection system based on machine vision is employed in the automatic line to detect cell sheet defect and to improve product quality.

To inspect the quality of the LiPo cell sheets during the production process, machine vision technique is employed in the system. We capture the images of two sides of these lithium-ion polymer cell sheets with controlled manipulators in the automatic product line as shown in Fig.1 and Fig. 2. After analyzing the defects of LiPo cell sheets carefully, these defects are classified into 4 categories. They are tab defects, separator defects, scratch defects and bubble defects as shown in Fig. 3. It is easy to detect tab defects, separator defects and scratch defects with machine vision techniques. However, it is difficult to detect bubble defects with the common methods, for their variety of background, size and height as shown in Fig. 4. We will propose a novel bubble defects detection method employing STM method with these captured LiPo cell sheets images. We will discuss STM theory in the following section.

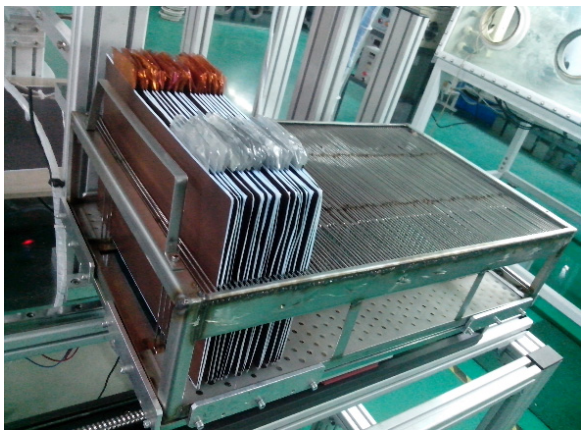

Fig. 1. The produced LiPo cell sheets to be checked.

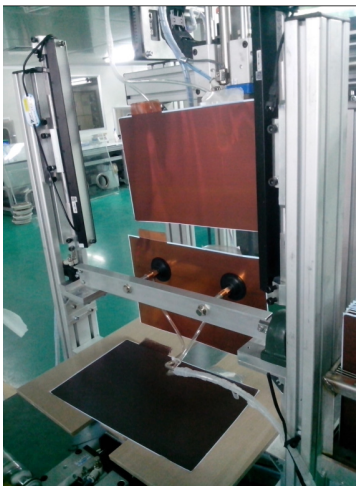

Fig. 2 Image caption of both sides of LiPo cell sheets with machine vision.

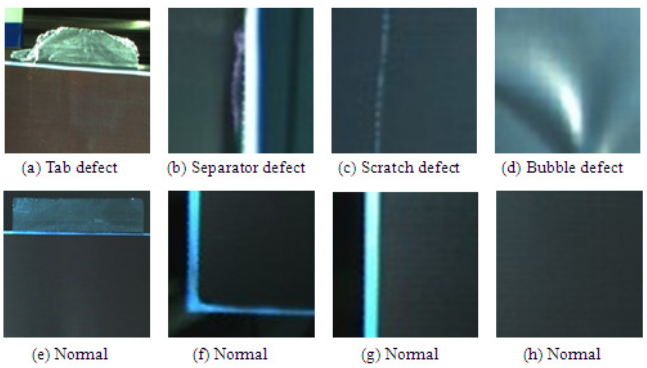

Fig.3 Defect and normal images of LiPo cell sheets. (a)-(d) are some typical defect images, and (e)-(h) are some normal images.

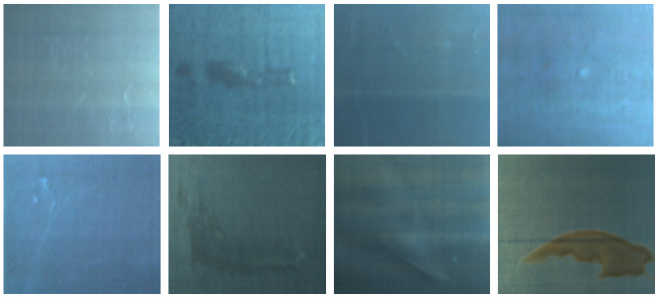

Fig. 4 Bubble defect image samples of dataset

III. Support Tucker Machines

In this section, we will review support Tucker machines theory which is employed for defect detection in the next section.

An n-th order tensor is an n-dimensional array. For a tensor $\boldsymbol{A}$, the i-th row of the j-th mode is denoted by $A_{(j)i:}$. The weights tensor $\boldsymbol{W}$ in the STM classifier is obtained from the Tucker tensor decomposition. The Tucker tensor decomposition of an M-th order tensor, $\boldsymbol{W} \in \mathbb{R}^{I_1 \times I_2 \times \cdots \times I_M}$, can be written as

$$\begin{aligned} \boldsymbol{W} &= \boldsymbol{G} \times_1 A^{(1)} \times_2 A^{(2)} \times \cdots \times_M A^{(M)} \\ &= \left[\!\left[\boldsymbol{G}; A^{(1)}, A^{(2)}, \cdots, A^{(M)} \right]\!\right] \end{aligned} \tag{1}$$

where $\boldsymbol{G}$ is a core tensor and $A^{(1)}, \cdots, A^{(M)}$ are a series of matrices that are multiplied to $\boldsymbol{G}$ along each mode. The optimization problem can be expressed as

$$\min_{\boldsymbol{G}, A^{(1)}, \ldots, A^{(M)}} = \left\| \boldsymbol{W} - \left[\!\left[\boldsymbol{G}; A^{(1)}, A^{(2)}, \cdots, A^{(M)} \right]\!\right] \right\| \tag{2}$$

s.t. $\boldsymbol{G} \in \mathbb{R}^{R_1 \times R_2 \times \cdots \times R_M}$, $A^{(n)} \in \mathbb{R}^{I_n \times R_n}$, $n = 1, \ldots, M$

Suppose that there is a dataset composed of L samples, denoted by $\boldsymbol{X} \in \mathbb{R}^{I_1 \times I_2 \times \cdots \times I_{M+1}}$. Each sample which belongs to one of the two classes Q_1 and Q_2 is a M-order tensor, denoted by $\boldsymbol{X}_{i_n} \in \mathbb{R}^{I_1 \times I_2 \times \cdots \times I_M}$, $i_n = 1, 2, \ldots, L$.

The objective of STM is to find a multi-linear function $g : \mathbb{R}^{I_1 \times I_2 \times \cdots \times I_M} \to [-1, 1]$. STM classifies the test tensor $\boldsymbol{Y} : \mathbb{R}^{I_1 \times I_2 \times \cdots \times I_M}$ in the test process by

$$g(\boldsymbol{Y}) = sign\left(\langle \boldsymbol{Y}, \boldsymbol{W} \rangle + b \right) \tag{3}$$

The tensor $\boldsymbol{W}$ formed by the weights parameters is obtained by calculating the following minimization problem:

$$\min_{\boldsymbol{W}, b, \xi \geq 0} \frac{1}{2} \langle \boldsymbol{W}, \boldsymbol{W} \rangle + c \sum_{i=1}^{I_{M+1}} \xi_i \tag{4}$$

$$\text{s.t. } y_i \left[\langle \boldsymbol{W}, \boldsymbol{X}_{i:} \rangle + b \right] \geq 1 - \xi_i, \; 1 \leq i \leq I_{M+1}, \xi_i \geq 0$$

where b is the bias term, $\xi = [\xi_i, \ldots, \xi_w]$ is the slack variable vector; and c is the penalty parameter which controls the degree of penalizing the misclassification of training samples. As the parameters in $\boldsymbol{W}$ are not all convex, we use an iterative method that we only solve the parameters correlated with the j-th mode of the weights tensor $\boldsymbol{W}$ (e.g. $W_{(j)}$) while keeping the other parameters constant.

The Kronecker product is defined as $A_{\otimes} = A^N \otimes \cdots \otimes A^{(1)}$. According to the weights tensor $\boldsymbol{W}$ obtained by the Tucker tensor decomposition of (1), the optimization problem defined in (4) can be rewritten as

$$\min_{A^{(j)}, b, \xi \geq 0} \frac{1}{2} \mathrm{Tr}\left[A^{(j)} G_{(j)} A_{\otimes}^{(j)^T} A_{\otimes}^{(j)} G_{(j)}^T (A^{(j)})^T \right] + c \sum_{i=1}^{I_{M+1}} \xi_i \tag{5}$$

$$\text{s.t.} \quad y_i \left[\mathrm{Tr}\left(A^{(j)} G_{(j)} A_{\otimes}^{(j)^T} X_{(j)i:}^T \right) + b \right] \geq 1 - \xi_i,$$

$$1 \leq i \leq I_{M+1}, \xi_i \geq 0$$

For using the SVM that is based on vector to solve the above problem, we set $P^{(j)} = A_{\otimes}^{(j)} G^{(j)}$, $K = P^{(j)} P^{(j)^T}$, $\tilde{A}^{(j)} = A^{(j)} K^{\frac{1}{2}}$, and $\tilde{X}_{(j)i:} = X_{(j)i:} P^{(j)} K^{\frac{1}{2}}$. And also, we let $\mathrm{Tr}\left[\tilde{A}^{(j)} (\tilde{A}^{(j)})^T \right] = \mathrm{vec}(\tilde{A}^{(j)})^T \, \mathrm{vec}(\tilde{A}^{(j)})$, $\mathrm{Tr}\left[\tilde{A}^{(j)} \tilde{X}_{(j)i:}^T \right] = \mathrm{vec}\left(\tilde{A}^{(j)} \right)^T \mathrm{vec}\left(\tilde{X}_{(j)i:} \right)$. Then the j-th mode of the optimization problem can be expressed as a SVM problem concerning $\tilde{A}^{(j)}$. The optimal $A^{(j)}$ can be found at the saddle point of the Lagrangian. It's calculated by

$$\begin{aligned} \mathrm{L}_{STMS}^{(j)}(A^{(j)}, b, \xi) &= \frac{1}{2} Tr\left[A^{(j)} P^{(j)} P^{(j)} (A^{(j)})^T \right] + c \sum_{i=1}^{I_{M+1}} \xi_i \\ &- \sum_{i=1}^{I_{M+1}} \alpha_i^j \left(y_i \left[Tr(A^{(j)} P^{(j)} X_{(j)i:}^T) + b \right] - 1 + \xi_i \right) - \sum_{i=1}^{I_{M+1}} \kappa_i \xi_i \end{aligned} \tag{6}$$

$$A^{(j)} = \sum_{i=1}^{I_{M+1}} \alpha_i^j y_i X_{(j)i:} P^{(j)} \left[P^{(j)} P^{(j)^T} \right]^{-1} \tag{7}$$

Lagrange multiplier α_i^j is obtained by solving the dual problem in (6). Through repeated iteration along each mode, we can calculate $A^{(j)}$, $j = 1 \ldots M$.

After getting $A^{(1)}, \ldots, A^{(N)}$, we will solve the core tensor $\boldsymbol{G}$. The minimization problem can be solved to obtain $\boldsymbol{G}$ as follow

$$\min_{G_{(1)}, b, \xi \geq 0} \frac{1}{2} \left(A_{\otimes} \, \mathrm{vec}(G_{(1)}) \right)^T \left(A_{\otimes} \, \mathrm{vec}(G_{(1)}) \right) + c \sum_{i=1}^{I_{M+1}} \xi_i \tag{8}$$

$$\text{s.t. } y_i \left[\left(A_{\otimes} \, \mathrm{vec}(G_{(1)})^T \right) \mathrm{vec}(X_{(j)i:}) + b \right] \geq 1 - \xi_i,$$

$$1 \leq i \leq I_{M+1}, \xi_i \geq 0 \tag{9}$$

where $\mathrm{vec}(G_{(1)})$ means the first dimension of the matrix form of $\boldsymbol{G}$, appearing as a vector. As $Q = A_{\otimes}^T A_{\otimes}$, $\tilde{V} = Q^{\frac{1}{2}} \mathrm{vec}(G_{(1)})$, $\tilde{X}_{(j)i:} = Q^{-\frac{1}{2}} X_{(j)i:}$, formula (8) can be written as

$$\min_{G_{(1)}, b, \xi \geq 0} \frac{1}{2} \mathrm{vec}(\tilde{V})^T \, \mathrm{vec}(V) + c \sum_{i=1}^{I_{M+1}} \xi_i \tag{10}$$

$$\text{s.t. } y_i \left[\mathrm{vec}(\tilde{V}^T) \, \mathrm{vec}(\tilde{X}_{(j)i:}) + b \right] \geq 1 - \xi_i, 1 \leq i \leq I_{M+1}, \xi_i \geq 0 \tag{11}$$

The optimal $\boldsymbol{G}$ can be found at the saddle point of the Lagrangian

$$\begin{aligned} \mathrm{L}_{STMS}(\mathbf{G}, b, \xi) &= \frac{1}{2} \left[\mathrm{vec}(G_{(1)})^T A_{\otimes}^T A_{\otimes} \, \mathrm{vec}(G_{(1)}) \right] + c \sum_{i=1}^{I_{M+1}} \xi_i \\ &- \sum_{i=1}^{I_{M+1}} \alpha_i \left(y_i \left[\mathrm{vec}(G_{(1)})^T A_{\otimes} \, \mathrm{vec}(X_{(j)i:}) + b \right] - 1 + \xi_i \right) - \sum_{i=1}^{I_{M+1}} \kappa_i \xi_i \end{aligned} \tag{12}$$

$$\mathrm{vec}(G_{(1)}) = \frac{1}{2} \sum_{i=1}^{I_{M+1}} \alpha_i y_i \left[A_{\otimes}^T A_{\otimes} \right] X_{(j)i:} \tag{13}$$

After solving the dual problem of (12), we can find the Lagrangian multipliers α_i.

IV. STM Based Defect Detection

The dataset of the Lithium-ion polymer cell sheets is captured from the automatic LiPo battery production line as described in Section 2, and some samples of the bubble defect are illustrated in Fig.4. We randomly select 200 Lithium-ion polymer cell sheet images from the dataset, and 100 images of them are with bubble defect and others without defect. The first step is to convert these colour images to gray images after the cell sheet net part is segmented from the entire image employing the edge detection algorithm in the colour image. Afterward we use the mean filter in spatial domain and Gaussian filter in frequency domain in the images, respectively, and we can obtain the subtract result images from the two filtered images. This filter method can eliminate noise to make the defects more obvious, and the surface reflective disturbances of LiPo cell sheets can be decreased. Finally we save all the images with the size of 50×50 to employ STM methods for bubble defect detection. The defect images are labelled as 1 while others are labelled as -1.

Compared to SVM and other similar classification methods, tensors those are employed in the STM algorithm are able to discover the hidden structure and potential information from the data with high dimensions. The stacked source images are typical nature high dimension data. When we use STM to these image data, we can obtain superior classification performance to other two-dimension array based methods. With the above STM theory, we can use STM for tensor classification in our defect detection application. Therefore we develop a bubble defect detection algorithm with the STM classifier. The classification method employing STM is realized as follows.

Inputs: train_data and test_data, the training data and the testing data; train_labels and test_labels, the labels of the training data and the testing data; epsilon, the threshold criterion; number_of_iterations, the maximum number of iterations; Rank, the rank of the tensor.
Outputs: acc, the accuracy of the classification for the testing data.
Steps:

1:randomly initialize U and G; iter=0
2:while iter<=number_of_iterations && tor>=epsilon
3: iter= iter+1
4: for j=1:2
5: U_old=U
6: $P^{(j)} = A_{\otimes}^{(j)} G^{(j)}$
7: $\mathrm{Vec}\left(\tilde{X}_{(j)i:}\right) = X_{(j)i:} \times P^{(j)T} \times (P^{(j)} \times P^{(j)T})^{-\frac{1}{2}}$
8: d=data($\tilde{X}_{(j)}$);
9: d.Y=train_labels'
10: [r,net]=train(svm(kernel('linear'), 'optimizer="andre"'},d))
11: w=get_w(net)
12: U{j}= reshape(w', [size(train_data,j) Rank]) $\times (P^{(j)} \times P^{(j)T})^{-\frac{1}{2}}$
13: end
14: dg=data($_{A_{\otimes}} \mathrm{Vec}\left(X_{(1)}\right)$)
15: dg.Y=train_labels'
16: [r,netg]=train(svm(net,dg))
17: wg=get_w(netg)
18: G_new = tensor(reshape(wg', [Rank Rank]))
19: b=netg.b0
20: TenUold=full(ttensor(tensor(G),U_old))
21: tenU=full(ttensor(tensor(G_new),U))
22: norm_u = norm(ten_U)
23: norm_u_gap = norm(tenU - tenUold)
24: tor = norm_u_gap/norm_u
25: G=G_new;
26:end
27: for n = 1 : N
28: Xdata = test_data(:,:,n)
29: pred(n) = innerprod(Xdata, tenU)
30: end
31:w_test=pred+b
32:pos=find(dec_values>0)
33:neg=find(dec_values<0)
34:predictions(pos)=1
35:predictions(neg)=-1
36:acc=100*length(find(predictions==test_labels))/length(test_labels)

V. Results and Discussion

In this section, we classify the LiPo cell sheet bubble defect with the proposed STM algorithm under Matlab R2013. The evaluation result may be influenced by the dataset which is a small-sample set, for that reason the cross-validation is used. The dataset is stochastically divided into two groups for cross-validation. Multiple grouping can make the limited data reuse to get the better estimation. The training data and testing data are randomly distributed by 4-fold cross validation. All samples are equally divided into four parts, in which one is used as testing data and others as training data.

It has been widely validated that neural network based classification has poor performance than SVM based one, and the references have also revealed that PCA based SVM is able to obtain high performance than SVM method [8]-[11]. Therefore, three methods are assessed in our experiments to verify the efficiency of our proposed method. They are SVM, PCA based SVM and our proposed STM method. After testing the different parameters with experiments, we select the optimized parameters for the best performance from the allowed ranges employing optimization search. We optimized the STM parameters as follows, the maximum number of iterations is 3, epsilon is 0.01, and rank is 4.

The comparisons of classification performance in a variety of sample number are performed. Total sample is selected from 10 to 100 with the step of 10. Half of the sample is randomly selected from the prepared bubble defect images, and the other half without defect. The comparison of classification correction rate is illustrated in Fig.5.

As shown in Fig.5, the classification accuracy of the proposed STM method is between 97.5% and 100%. With the increase of training samples, the classification accuracy gradually increases as well. The classification accuracy is more prior to other two methods when less training samples are employed. With the sample number increasing, the classification accuracy of the proposed STM method is evidently higher than SVM method. And it also gives an advantage over PCA based SVM method, although they have the similar accuracy when the number of sample is 70 and 80. However, the accuracy of the PCA based SVM method decreases with fewer samples while our proposed method is able to keep the superior performance of accuracy. It means that our proposed STM method has most satisfactory performance with varies of sample number.

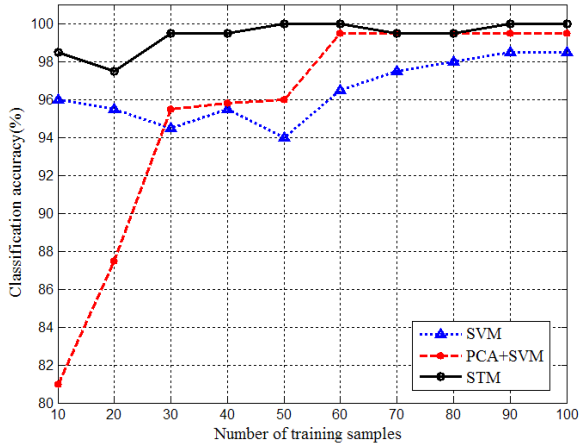

Fig. 5 Defect detection classification accuracy of different methods

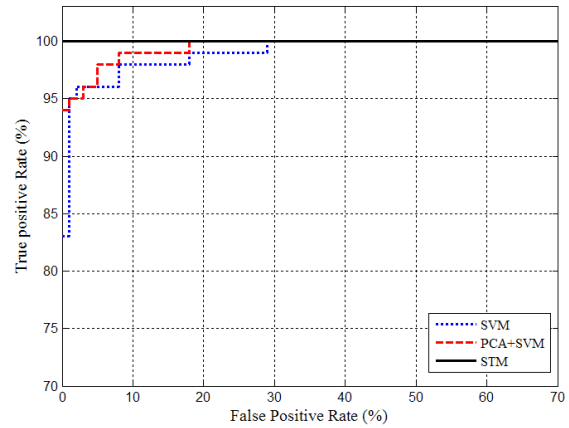

(a) sample number= 30

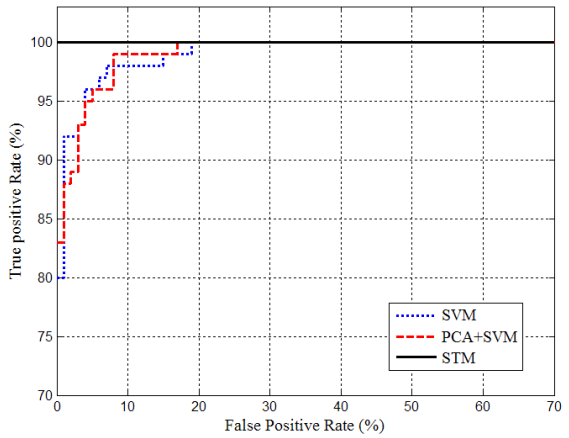

(b) sample number= 50

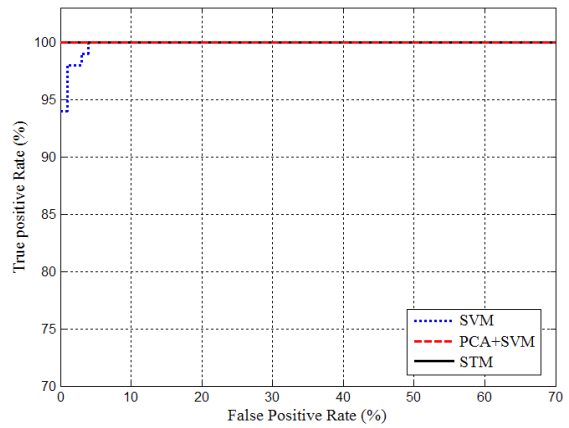

(c) sample number= 70

Fig. 6 Comparison of ROC and AUC with different sample number

TABLE I
AUC OF DIFFERENT METHODS

Sample Number	SVM	PCA-SVM	STM
10	0.9925	0.9822	0.9998
20	0.9909	0.9795	0.9995
30	0.9923	0.9960	1
40	0.9923	0.9955	1
50	0.9926	0.9927	1
60	0.9980	0.9999	1
70	0.9989	1	1
80	0.9990	1	1
90	0.9993	1	1
100	0.9993	1	1

Receiver operating characteristics (ROC) curve and Area under the ROC curve (AUC) are widely used for classification performance comparison, and they are also employed in our experiments. We set the threshold varying from maximum to minimum and get the ROC curve. Interpreted as the probability that a classifier is able to distinguish a randomly chosen positive instance from a randomly chosen negative instance, AUC value is bigger when the classification has good performance. AUC is listed in Table 1 where three different classification methods and different sample number are evaluated.

When the training sample number increases, STM can rapidly reach the best classification performance with merely 30 training samples while PCA based SVM method increases to the best performance gradually with 70 samples. And SVM method is too slow to obtain the accuracy of 100% after sample number has reached 100.

The detailed ROC curve and AUC are illustrated in Fig. 6. SVM method, PCA based SVM method and our proposed STM method are compared in the illustration where the sample number is selected as 30, 50 and 70, respectively. It is obvious that the illustration is consistent with the data in Table 1 and our analysis above. All these experiments have shown that our proposed STM based method has the best performance.

VI. CONCLUSIONS

In this work, we applied STM classification to detect bubble defect of LiPo cell sheets with machine vision technology. Compared with other learning based classifiers, our proposed STM based method can obtain better performance. This reveals that tensor based STM is an effective classification method applied to image problem, for it can retain the original structure information and relationship of the images. Research of the more efficient automatic parameter optimization method for STM will be carried out in the future.

REFERENCES

[1] A. M. Stephan and K.S. Nahm, "Review on composite polymer electrolytes for lithium batteries", *Polymer,* vol. 47, no. 16, pp5952-5964, 2006.

[2] H.G. Bu, J. Wang and X.B. Huang, “Fabric defect detection based on multiple fractal features and support vector data description”, *Engineering Applications of Artificial Intelligence*, vol. 22. no. 2, pp224-235, 2009.

[3] S. Nashat, A. Abdullah and M.Z. Abdullah, “Machine vision for crack inspection of biscuits featuring pyramid detection scheme”, *Journal of Food Engineerin*g, vol. 120, no. 1, pp233-247, 2014.

[4] C.C. Wang, B.C. Jiang, J.Y. Lin and C.C. Chu. “Machine Vision-Based Defect Detection in IC Image Using the Partial Information Correlation Coefficient”. *IEEE Trans. Semiconductor Manufacturing*, vol. 26, no. 3, pp378-384, 2013.

[5] M. Israil, S.A. Anwar and M.Z. Abdullah, “Automatic detection of micro-crack in solar wafers and cells: a review”, *Trans. the Institute of Measurement and Control*, vol. 35, no. 5, pp606-618, 2013.

[6] D. Weimer, H. Thamer and B. Scholz-Reiter, “Learning defect classifiers for textured surfaces using neural networks and statistical feature representations”, *Proc. 46th CIRP Conf. Manufacturing Systems*, Setubal, Portugal, Portugal, 2013, pp347-352.

[7] S. Nashat, A, Abdullah, S; Aramvith and M.Z. Abdullah, “Support vector machine approach to real-time inspection of biscuits on moving conveyor belt”. *Computers and Electronics in Agriculture*, vol. 75, no. 1, pp147-158, 2011.

[8] R. Shanmugamani, M. Sadique and B. Ramamoorthy, “Detection and classification of surface defects of gun barrels using computer vision and machine learning”. *Measurement: Journal of the International Measurement Confederation*, vol. 60, pp. 222-230, 2015.

[9] W. Mu, J. Gao, H. Jiang, Z. Wang, F. Chen and C. Dang, "Automatic classification approach to weld defects based on PCA and SVM", *Insight: Non-Destructive Testing and Condition Monitoring*, vol. 55, no. 10, pp535-539, 2013

[10] S. Raj and K.C. Ray, "A comparative study of multivariate approach with neural networks and support vector machines for arrhythmia", *Proc. International Conf. Energy, Power and Environment* (ICEPE), India, 2015, articel no. 7510156.

[11] P. Govender and N. Pillay, "Support vector machine classification and sorting system for cigarette brands," *Lecture Notes in Engineering and Computer Science: Proceedings of the. World Congress on Engineering* 2014, WCE 2014, 2-4 July, 2014, London, U.K., pp577-581.

[12] D. Tao, X. Li, X. Wu and W. Hu, “Supervised tensor learning”, *Knowledge and Information Systems*, vol. 13, no. 1, pp1-42, 2007.

[13] I. Kotsia and I. Patras, “Support Tucker Machines”, *Proc. IEEE Conf. Computer Vision and Pattern Recognition* (CVPR), Colorado, 2011, pp633-640.

[14] L. Ma, “Support Tucker machines based marine oil spill detection using SAR images”, Indian Journal of Geo-Marine Sciences, vol. 45, no. 11, pp1445-1449, 2016.